Volume 20, No 1 | International Journal of Radiation Research, January 2022

A study of MRI-based machine-learning methods for glioma grading

Z. Wang[1], X. Xiao[1*], K. He[1], D. Wu[2], P. Pang[3], T. Wu[4]

[1]*Department of Radiology, Second Affiliated Hospital of Nanchang University, Nanchang, China*
[2]*Department of Radiology, First Affiliated Hospital of GanNan medical college, GanNan, China*
[3]*Life Sciences, GE Healthcare, Hangzhou, China*
[4]*Life Sciences, GE Healthcare, Shanghai, China*

► ***Original article***

***Corresponding author:**
Xinlan Xiao, Ph.D.,
E-mail:
jx_xiaoxinlan@sina.com

Received: October 2020
Final revised: January 2021
Accepted: February 2021

Int. J. Radiat. Res., January 2022; 20(1): 115-120

DOI: 10.52547/ijrr.20.1.18

Keywords: *MRI, Radiomics, glioma, machine-learning method.*

ABSTRACT

Background*:** Preoperative classification of gliomas is essential to identify the optimal treatment and prognosis. The aim of this study was to identify the optimal machine learning methods that can be used to accurately grade gliomas based on magnetic resonance images (MRI). ***Materials and Methods: A total of 153 glioma patients from two medical institutions were enrolled. Four methods, namely support vector machine -recursive feature elimination (SVM-RFE), least absolute shrinkage and selection operator (LASSO), max-relevance and min-redundancy (mRMR), and decision trees were used to screen glioma features. Five follow-up classifiers, including decision trees (DT), naive Bayes (NB), K-Nearest Neighbor (KNN), logistic regression (LR), and the support vector machine (SVM), were then used to develop the models. Receiver operating characteristic (ROC) curves were then plotted, and the area under the curve (AUC) was calculated to evaluate the prediction performance of the models. The accuracy, sensitivity, and specificity of the models were also calculated. ***Results:*** A total of 1070 predictive features based on image histograms, shape, and texture were extracted from preoperative T1-weighted contrast-enhanced imaging (T1-CE) MRI scans. The SVM-RFE and SVM models yielded the highest prediction performance with an AUC, sensitivity, specificity, and accuracy of 0.985, 94.2%, 89%, and 91.1%, respectively, while LASSO and NB had the lowest accuracy, with an AUC, sensitivity, specificity, and accuracy of 0.854, 97.9%, 72.3% or 85.1%, respectively. The average AUC and accuracy for the four methods were SVM-RFE (0.967, 91.3%), LASSO (0.951, 88.1%), mRMR (0.935, 90%), and DT (0.954, 90.4%). In the validation cohort, the average AUC and accuracy were SVM-RFE (0.837, 80%), LASSO (0.786, 76.6%), mRMR (0.817, 82.2%) and DT (0.70, 71.1%). ***Conclusion:*** The radiomics models could yielded a good performance in differentiating LGG from HGG, and the SVM-RFE combined with other machine-learning methods could provide the best average performance.

INTRODUCTION

Gliomas are the most common malignant tumors of the central nervous system (CNS). Based on the world health organization (WHO) pathological grading criteria, grades I to II are classified as low-grade gliomas (LGG), and grades III to IV are classified as high-grade glioma (HGG). Grading of brain gliomas affects the patient treatment strategy and prognosis [1-4]. Therefore, preoperative evaluation of brain glioma grade is extremely important in the management of glioma patients. Histopathological assessment after surgery or biopsy is still considered the gold standard for glioma grading. However, surgery is an invasive procedure and may not always be feasible. Therefore, multi-modality magnetic resonance imaging (MRI) techniques are widely used to facilitate preoperative grading of glioma.

MRI is a non-invasive imaging technique that plays a pivotal role in the diagnosis of gliomas [5]. However, MRI does not always fully reflect the physiological and pathological characteristics of the tumor [6]. Furthermore, the traditional interpretation of MRI can be subjective as it relies on a visual assessment and semi-quantitative descriptive parameters. Advanced radiomics techniques are now being developed to facilitate the quantitative assessment and reduce the subjectivity in imaging interpretation. These quantitative features can also be used to assess invisible tumor biological information such as heterogeneity, angiogenic characteristics, infiltration, and metastasis. However, the successful implementation of these models in clinical practice highly depends on the ease of use and prediction accuracy of these models.

Radiomics involves the quantitative extraction of features such as shape, texture, and histograms from

medical images representing structural, physiopathologic, and genetic characteristics. Machine-learning (ML) models are then used to interpret the image features and produce clinically relevant information. ML can simulate or mimic human learning behavior to acquire new knowledge or skills or to reorganize the existing knowledge structure to further improve its own performance [7]. Various machine learning techniques have been developed, and these vary considerably in efficiency and accuracy.

Various imaging sequences can be used to facilitate the diagnosis of brain tumors. Fouke *et al.* [8] suggest that patients with a suspected brain tumor should be first scanned using T1-weighted imaging (T1W1), T2-weighted imaging (T2W1), and gadolinium-based contrast-enhanced T1-weighted image (T1-CE). However, previous radiomics studies showed that T1-CE has better predictive performance when compared with other sequences for grading gliomas [9, 10].

At present, many imaging studies have made use of radiomics technology to compare the accuracy of the different MRI sequences in predicting tumor prognosis [9,10]. However, these studies tended to make use of only one feature-reduction or classification method to characterize the tumor, limiting the accuracy of these models. Therefore, this study aimed to extract a large spectrum of features predictive of glioma from the T1-CE MRI sequence. The secondary objective of the study was to test and validate the predictive performance of various ML models using different classification methods, expecting that the results will provide a useful reference for researchers related.

MATERIALS AND METHODS

Participants

The study was performed in accordance with the 1964 Helsinki declaration and its later amendments or comparable ethical standards. All procedures involving human participants were approved by the Second Affiliated Hospital of Nanchang University Medical Research Ethics Committee (Jiangxi, China) [No. Review [2020] No. (033); the number of cases: 153; start-stop time: 2020.06-2020.11]. All patients with brain glioma who underwent a routine MRI examination within a week before surgery at two medical institutions from July 2017 to May 2020 were analyzed. All patients had a histopathological confirmation of the glioma grade according to the World Health Organization (WHO) classification of CNS tumors. None of the patients had undergone radiotherapy or chemotherapy treatment before the operation. Patients were excluded from the study if they had; poor quality images that could not meet the software post-processing requirements, recurrent gliomas, brain hemorrhage, and those who had puncture biopsy before surgery.

MRI scanning parameters

All patients underwent a multi-sequence imaging protocol on a 3.0 Tesla MRI system (Discovery 750, GE Healthcare, Milwaukee, WI), with an 8-channel head coil (GE Medical Systems) using a T1-weighted spin-echo image (T1WI), a repetition echo time ratio (TR/TE) of 1,750/25.4 msec, a matrix size of 512×512, a field of view (FOV) of 24×24 cm^2, a slice thickness of 5 mm with a gap of 1.5 mm and an acquisition time of 1 minute and 29 seconds. An additional T1WI sequence was acquired after a bolus injection of 0.1 mmol/kg of gadodiamide (Omniscan, GE Healthcare, Cork, Ireland) to obtain the T1-CE image.

Definition of the region of interest (ROI)

ITK-snap software (www.itksnap.org) was used for manual image segmentation. T1-CE images were selected for ROI sketch, the ROI delineation was determined by the enhancement region of tumor, and it carried out by two senior radiologists with more than ten years of work experience using double-blind method. In case of any disagreement on the position of the ROI, a consensus was reached by discussion, especially if the positional variations resulted in a discrepancy.

Feature extraction

The GE-IF (Intelligence Foundry, GE medical) analysis software based on pyradiomics (python 3.7.3) and matplotLab 3 was used to automatically identify and extract 1070 imaging features from the T1-CE images (table 2, part2 of figure 2).

Feature Selection and Model establishment

According to the ratio of 8:2,129 images were randomly divided into training and validation datasets. The LGG group was labeled as "0" while the HGG group was labeled as "1". The missing values were filled using the median. The synthetic minority oversampling technique (SMOTE) [11] was used for sample balancing, and Z-score standardization was used to normalize the data [12] (parts 2 to 3 of figure 2). Four feature-reduction methods, namely support vector machine-recursive feature elimination (SVM-RFE), least absolute shrinkage and selection operator (LASSO), max-relevance and min-redundancy (mRMR), and decision trees were used to screen glioma features. Five follow-up classifiers, including decision trees (DT), naive Bayes (NB), K-Nearest Neighbor (KNN), logistic regression (LR), and the support vector machine (SVM), were then used to develop the models as indicated in parts 4 to 5 of figure 2.

Model evaluation

For both training and validation datasets, receiver

operating characteristic (ROC) curves were plotted, and the area under the curve (AUC) was calculated to evaluate the prediction performance of the models. The accuracy, sensitivity, and specificity of the models were also calculated.

Statistical analysis

The statistical package for the social sciences (SPSS) software version 22.0 (IBM, Armonk, NY, USA) was used for data analysis. The quantitative data were summarized as mean ± standard deviation. The independent sample t-test was used to compare the differences between the two groups. The chi-squared test was used to identify whether there was a statistically significant difference in the gender between the LGG and HGG. The reported statistical significance levels were all two-sided, with statistical significance set at 0.05.

RESULTS

After rigorous screening, 129 cases met the inclusion criteria, of which 50 were LGG while 79 were HGG. The study cases included 83 men and 46 women, aged from 20 to 81 years old. (table1, figure 1). There was a statistically significant difference in age between the LGG (mean: 42.32 years±16.51) and HGG (mean: 52.75 years±13.10) groups (P<0.01), but the difference in gender was not statistically significant.

The prediction models were established by different classifiers. For the single model, the SVM-RFE and SVM model had the highest prediction performance in the training cohort with an AUC, sensitivity, specificity, and accuracy of 0.985, 94.2%, 89%, and 91.1%, respectively. On the other hand, the prediction efficiency for LASSO with NB was the lowest in the training cohort, with an AUC, sensitivity, specificity, and accuracy of 0.854, 97.9%, 72.3%, and 85.1%, respectively (figure 3, table 3). The AUC and accuracy comparison between each model is further illustrated in Fig 4. In the training cohort, the average AUC and accuracy for the four models were: SVM-RFE (0.967, 91.3%), LASSO (0.951, 88.1%), mRMR (0.935, 90%), and DT (0.954, 90.4%). In the validation cohort, the average AUC and accuracy for the four models were: SVM-RFE (0.837, 80%), LASSO (0.786, 76.6%), mRMR (0.817, 82.2%), and DT (0.70, 71.1%) (figure 5).

Table 1. Baseline demographic and clinical characteristics of the patients.

	Low Grade	High Grade	*P*-value
Patients (N/%)	38.7% (50/129)	61.3% (79/129)	NA
Age (mean ± SD)	42.32 ± 16.51	52.75 ± 13.10	<0.01
Gender (N/%)			0.754
Male	66.0% (33/50)	63.3% (50/79)	NA
Female	34.0% (17/50)	36.7% (29/79)	NA

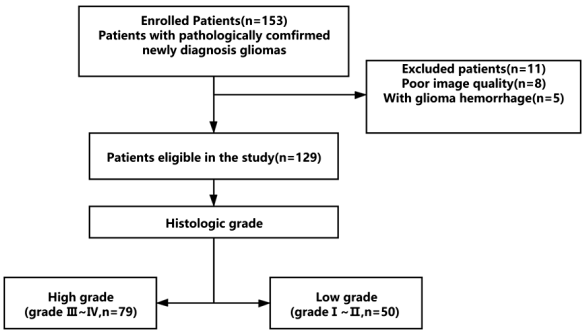

Figure 1. Flow diagram for patient selection and the main two main grading tasks in our study.

Table 2. Categories and abundance of the extracted features.

Category	Number
First Order Features	18
Shape Features	13
GLCM (Gray Level Co-occurrence Matrix)	23
Glrlm (Gray Level Run Length Matrix)	16
Glszm (Gray Level Size Zone Matrix)	16
Gtdm (Gray Tone Difference Matrix)	5
NGldm (Neighboring Gray Level Dependence Matrix)	13
Normalized_radial_lengths	3
Area ratio of macroscopic contour	1
Roughness index of boundary	1
Textural_phenotype	23
Ipris(Intra-perinodular Textural Transition)	48
CoLIAGe2D	456
Wavelet	434
Total	1070

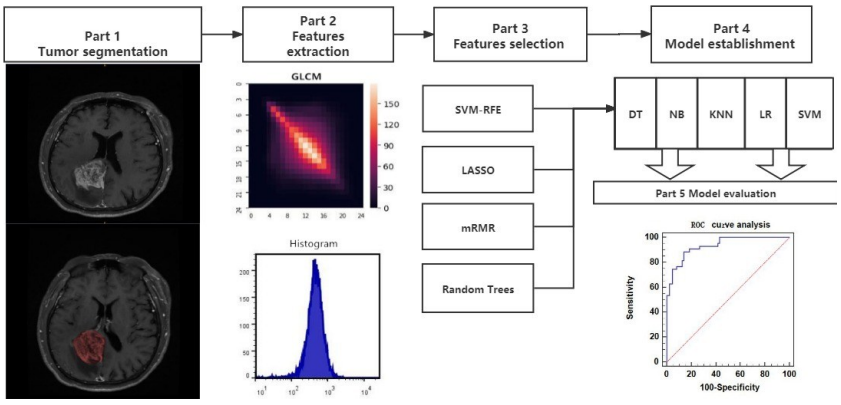

Figure 2. The main procedure of the proposed radiomics strategy for preoperative glioma grading. Part 1 shows the region of tumor (enhanced section) and segmentation of ROI (red section). Part 2, for e.g, Image feature like GLCM, Histogram were extracted. Part 3,four methods (SVM-RFE, LASSO, mRMR, Random Trees) were used for features selection and five methods (DT, NB, KNN, LR and SVM) below Part 4 were used for model establishment; Part 5, a ROC curve was used for model evaluation. Abbreviation for Fig 2: GLCM: Gray-level Co-occurrence Matrix; DT: Decision Trees; NB: Naive Bayes;KNN: K-Nearest Neighbor; LR: Logistic Regression; SVM: .Support Vector Machine.

Table 3. Classification performance of the LGG versus the HGG cohort using different feature selection modalities.

Model	Number of Features after screened	Performance	AUC	Sensitivity	Specificity	Accuracy
Spearman0.95+SVM-RFE+KNN	16	Training	0.972	0.894	0.936	0.915
		Validation	0.861	0.833	0.667	0.778
Spearman0.95+SVM-RFE+Naive Bayes	15	Training	0.935	0.979	0.787	0.883
		Validation	0.986	0.917	0.833	0.889
Spearman0.95+SVM-RFE+Logistics Regression	15	Training	0.983	0.955	0.916	0.920
		Validation	0.861	0.917	0.667	0.833
Spearman0.95+SVM-RFE+SVM	13	Training	0.985	0.942	0.890	0.911
		Validation	0.75	0.917	0.333	0.722
Spearman0.95+SVM-RFE+Decision Tree	19	Training	0.962	0.915	0.957	0.936
		Validation	0.729	0.917	0.5	0.778
Spearman0.95+LASSO+SVM	23	Training	0.980	0.905	0.926	0.912
		Validation	0.847	0.917	0.667	0.833
Spearman0.95+LASSO+Naive Bayes	19	Training	0.854	0.979	0.723	0.851
		Validation	0.764	0.75	0.667	0.722
Spearman0.95+LASSO+Logistics Regression	17	Training	0.977	0.923	0.918	0.896
		Validation	0.819	0.833	0.833	0.833
Spearman0.95+LASSO+KNN	17	Training	0.964	0.957	0.809	0.883
		Validation	0.958	1.0	0.5	0.833
Spearman0.95+LASSO+Decision Tree	15	Training	0.978	0.911	0.923	0.862
		Validation	0.542	0.75	0.333	0.611
mRMR+SVM	5	Training	0.975	0.936	0.936	0.936
		Validation	0.847	0.667	1.0	0.778
mRMR+Naive Bayes	5	Training	0.867	0.872	0.851	0.862
		Validation	0.847	0.917	0.833	0.889
mRMR+Logistics Regression	5	Training	0.885	0.894	0.787	0.84
		Validation	0.736	0.833	0.667	0.778
mRMR+KNN	5	Training	0.964	0.936	0.872	0.904
		Validation	0.778	0.917	0.5	0.778
mRMR+Decision Tree	5	Training	0.986	0.936	0.979	0.957
		Validation	0.875	0.917	0.833	0.889
Spearman0.95+Random Trees+Decision Tree	6	Training	0.969	1.0	0.766	0.883
		Validation	0.833	0.917	0.667	0.833
Spearman0.95+Random Trees+KNN	6	Training	0.947	0.915	0.851	0.883
		Validation	0.715	0.667	0.667	0.667
Spearman0.95+Random Trees+Logistics Regression	6	Training	0.949	0.915	0.915	0.915
		Validation	0.75	0.833	0.333	0.667
Spearman0.95+Random Trees+Naive Bayes	6	Training	0.928	0.915	0.809	0.862
		Validation	0.632	0.833	0.333	0.667
Spearman0.95+Random Trees+SVM	6	Training	0.978	0.979	0.979	0.979
		Validation	0.569	0.833	0.5	0.722

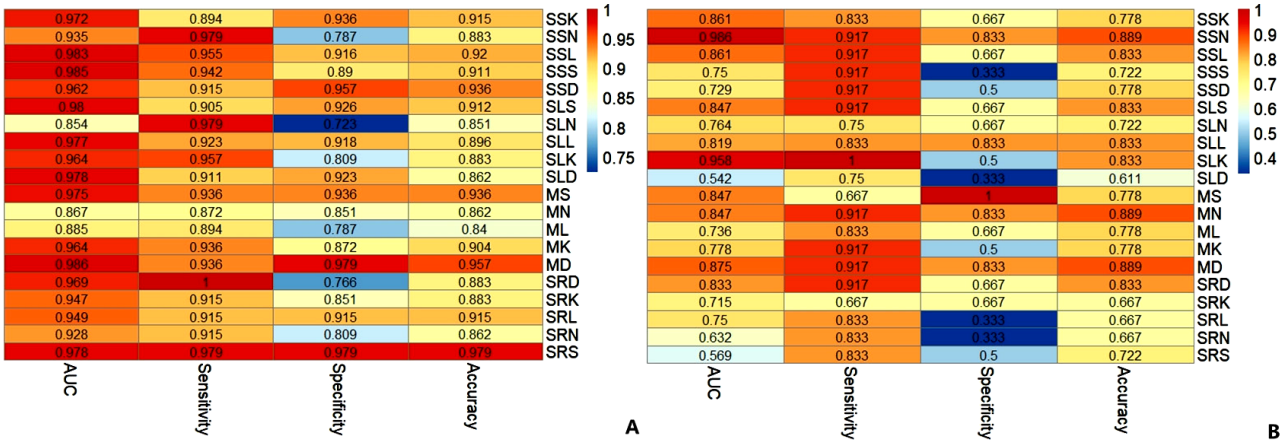

Figure 3. Heat map for the performance of various models in training **(A)** and validation **(B)** cohort Abbreviation for Figure 3: SSK,Spearman0.95+SVM-RFE+KNN; SSN,Spearman0.95+SVM-RFE+Naive Bayes; SSL,Spearman0.95+SVM-RFE+Logistics Regression; SSS, Spearman0.95+SVM-RFE+SVM;SSD,Spearman0.95+SVM-RFE+Decision Tree;SLS,Spearman0.95+LASSO+SVM; SLN,Spearman0.95+LASSO+Naive Bayes;SLL,Spearman0.95+LASSO+Logistics Regression;SLK; Spearman0.95+LASSO+KNN; SLD; Spearman0.95+LASSO+Decision Tree, MS; mRMR+SVM, MN; mRMR+Naive Bayes, ML; mRMR+Logistics Regression MK, mRMR+KNN; MD, mRMR+Decision Tree;SRD,Spearman0.95+Random Trees+Decision Tree; SRK,Spearman0.95+Random Trees+KNN;SRL,Spearman0.95+Random Trees+Logistics Regression; SRN,Spearman0.95+Random Trees+naïve Bayes; SRS; Spearman0.95+Random Trees+SVM.

DISCUSSION

Currently, MRI is the most commonly used imaging method for the diagnosis and monitoring of glioma. The main advantage of this imaging technology is that it provides quantitative data that can be used to assess mass-occupancy effects, edema, contrast enhancement, and necrosis. This information can be used to grade gliomas pre-operatively. Various machine learning models have been developed to facilitate the grading of gliomas, but sometimes the performance of prediction models is limited since they are often based on a limited number of features and a inappropriate feature selection method. In the study, we made use of four different feature extraction methods, including SVM-RFE, LASSO, mRMR, and DT, to extract 1070 glioma features from T1-CE images. Five follow-up ML classifiers, including DT, NB, KNN, LR, and SVM, were then used to develop predictive models.

Our findings indicate that models like LASSO with DT and RT with NB had high AUC values in the training dataset with a considerably lower AUC following validation. These models tend to be prone to over-fitting. Over-fitting occurs when the full model contains too many covariates relative to the amount of information (sample size and number of outcome events) in the sample [13]. As a result, the over-fitting model often appears to work well in the training set but poorly in the validation set. In other words, the generalization ability of the model is weak. In order to minimize the risk of over-fitting, the optimum number of hidden nodes was determined by adopting ten-fold cross-validation. Moreover, models with both high AUC and high accuracy in both training and validation datasets were selected to further minimize the risk of overfitting. The average performance of each group (SVM-RFE, LASSO, mRMR, RT) in both training and validation datasets was therefore compared, and the optimal model was selected (figure 5).

Support vector machines (SVM) is a powerful tool that can be used to analyze data with a number of predictors approximately equal to or larger than the number of observations [13] and can therefore be used for both feature selection and model building. It is, therefore, one of the most commonly used ML algorithms in tumor differentiation and gene selection [14,15]. SVM-RFE requires training of the SVM classifier with a linear kernel function and a computation of the ranking criterion for all features in order to identify and remove the smallest ranking criterion. Tian *et al.* adopted this method and combined it with radiomics for glioma grading. In this study, SVM achieved good prediction results [9], with a grading accuracy and an AUC of 89.2% and 0.946, respectively. On the other hand, Zhou *et al.* [16] used ML algorithms and achieved high accuracy in the prediction of isocitrate dehydrogenase 1 (IDH1) genotype in gliomas and moderate accuracy in a three-group prediction including IDH genotype and 1p19q co-deletion. In our study, most of the models constructed with SVM-RFE obtained optimal prediction performance.

LASSO and mRMR, and RT are the most commonly used feature reduction methods in radiomics with very high performance levels for the characterization of gliomas. Wang *et al.* used LASSO for feature extraction and selection, eventually achieving an AUC on T1-CE sequences of 0.914 in the training cohort [17]. Sun *et al.* [18] used mRMR to predict vascular endothelial growth factor (VEGF) expression in patients with diffuse gliomas based on radiomics, eventually achieving a AUC of 0.741 in the training group and 0.702 in the validation group.

In our study, we evaluated 20 different model combinations to identify the best performing models in the grading of gliomas. However, the main limitation of our study was the small sample size, which eventually led to over-fitting. Therefore, our future studies will loop in more data to improve the generalizability of the models. The models should be further optimized by selecting the best predictive features to minimize the over-fitting problem [19]. Furthermore, feature extraction was performed on T1-CE images only, other MRI sequences such as T1WI, T2WI, or apparent diffusion coefficient (ADC) sequences could potentially be used to extract additional predictive glioma features and hence improve the performance of the models. Not all classifiers were evaluated in our study. Other classifiers like principal component analysis (PCA) [20] and linear discriminant analysis (LDA) warrant further investigations as they were found to perform well in previous studies [21]. Finally, there is the need to develop models that can be used clinically to predict prognosis and facilitate therapeutic management based on various tumor characteristics.

CONCLUSION

The results suggest that based on the T1-CE sequence, these radiomics models could yielded a good performance in differentiating LGG from HGG. Among them,the SVM-RFE algorithm combined with other machine-learning method provided the best average predictive performance. Therefore, this model could provide a non-invasive tool to grade gliomas pre-operatively, eventually facilitating patient management.

ACKNOWLEDGMENT

We would like to thank Top Edit (www.topeditsci.com) for the English language editing of this manuscript.

Consent for publication: not applicable.

Availability of supporting data: The datasets analyzed during the current study are available from the corresponding author upon request.

Competing interests: The authors declare that they have no conflict of interest.

Conflicts of interest: *None declared.*

Funding: This work was supported and funded by the Key Research and Development Projects in Jiangxi Province, China, (NO.20171ACG70002).

Authors' contributions: Conceptualization: (ZW, XX, KH, DW, PP); Data curation: (ZW, DW); Formal analysis: (ZW, XX, KH, DW); Funding acquisition: (ZW, XX, KH, DW); Investigation: (ZW, XX); Methodology: (ZW, XX); Project administration: (ZW, XX, KH, DW, PP); Resources: (ZW, XX, KH, DW, PP); Software: (ZW, XX, KH, PP); Supervision: (ZW, DW); Validation: (ZW, DW); Visualization: (ZW, DW, PP); Writing – original draft: (ZW, DW, PP); Writing – review & editing: (ZW, DW, PP).

REFERENCES

1. Goya-Outi J, Orlhac F, Calmon R, Alentorn A, Nioche C, Philippe C, Puget S, Boddaert N, Buvat I, Grill J, Frouin V, Frouin F (2018) Computation of reliable textural indices from multimodal brain MRI: suggestions based on a study of patients with diffuse intrinsic pontine glioma. *Phys Med Biol,* ***63****(10): 105003*.
2. Wu W, Lamborn KR, Buckner JC, Novotny PJ, Chang SM, O'Fallon JR, Jaeckle KA, Prados MD (2010) Joint NCCTG and NABTC prognostic factors analysis for high-grade recurrent glioma. *Neuro-oncology,* ***12****(2): 164–172*.
3. Menze BH, Jakab A, Bauer S, Kalpathy-Cramer J, Farahani K, Kirby J, Burren Y, Porz N, Slotboom J, Wiest R, Lanczi L, Gerstner E, Weber MA, Arbel T, Avants BB, Ayache N, Buendia P, Collins DL, Cordier N, Corso JJ, Van Leemput K (2015) The multimodal brain tumor image segmentation benchmark (BRATS). *IEEE Trans Med Imaging,* ***34****(10), 1993–2024*.
4. Cho HH and Park HJ (2017) Classification of low-grade and high-grade glioma using multi-modal image radiomics features. *Conf Proc IEEE Eng Med Biol Soc, 3081–3084*.
5. Viallon M, Cuvinciuc V, Delattre B, Merlini L, Barnaure-Nachbar I, Toso-Patel S, Becker M, Lovblad KO, Haller S (2015) State-of-the-art MRI techniques in neuroradiology: principles, pitfalls, and clinical applications. *Neuroradiology,* ***57****(5): 441–467*.
6. Suh HB, Choi YS, Bae S, Ahn SS, Chang JH, Kang SG, Kim EH, Kim SH, Lee SK (2018) Primary central nervous system lymphoma and atypical glioblastoma: Differentiation using radiomics approach. *Eur Radiol,* ***28****(9): 3832–3839*.
7. Piccolo SR., Lee TJ, Suh E, Hill K. (2020) ShinyLearner: A containerized benchmarking tool for machine-learning classification of tabular data. *GigaScience,* ***9****(4): giaa026*.
8. Fouke SJ, Benzinger T, Gibson D, Ryken TC, Kalkanis SN, Olson JJ (2015) The role of imaging in the management of adults with diffuse low grade glioma: A systematic review and evidence-based clinical practice guideline. *J Neurooncol ,* ***125****(3) : 457–479*.
9. Tian Q, Yan LF, Zhang X, Zhang X, Hu YC, Han Y, Liu ZC, Nan HY, Sun Q, Sun YZ, Yang Y, Yu Y, Zhang J, Hu B, Xiao G, Chen P, Tian S, Xu J, Wang W, Cui GB (2018) Radiomics strategy for glioma grading using texture features from multiparametric MRI. *J Magn Reson Imaging,* ***48****(6): 1518–1528*.
10. Tan, Y., Zhang, S. T., Wei, J. W., Dong, D., Wang, X. C., Yang, G. Q., Tian, J., & Zhang, H. (2019). A radiomics nomogram may improve the prediction of IDH genotype for astrocytoma before surgery. Eur Radiol, 29(7), 3325–3337.
11. Blagus R and Lusa L (2013) SMOTE for high-dimensional class-imbalanced data. *BMC Bioinformatics,* ***14****: 106*.
12. Yasrebi H (2016) Comparative study of joint analysis of microarray gene expression data in survival prediction and risk assessment of breast cancer patients. *Briefings in Bioinformatics,* ***17****(5): 771–785*.
13. Sanz H, Valim C, Vegas E, Oller JM, Reverter F (2018) SVM-RFE: selection and visualization of the most relevant features through non-linear kernels. *BMC Bioinformatics,* ***19****(1), 432*.
14. Tan PL, Tan SC, Lim CP, Khor SE (2011) A modified two-stage SVM-RFE model for cancer classification using microarray data. *Lecture Notes in Computer Science, 668–675*.
15. Das P, Roychowdhury A, Das S, Roychoudhury S, Tripathy S (2020) Sigfeature: Novel significant feature selection method for classification of gene expression data using support vector machine and t statistic. *Frontiers in Genetics,* ***11****: 247*.
16. Zhou H, Chang K, Bai HX, Xiao B, Su C, Bi WL, Zhang PJ, Senders JT, Vallières M, Kavouridis VK, Boaro A, Arnaout O, Yang L, Huang RY (2019) Machine learning reveals multimodal MRI patterns predictive of isocitrate dehydrogenase and 1p/19q status in diffuse low- and high-grade gliomas. *J Neurooncol,* ***142****(2): 299–307*.
17. Wang Q, Li Q, Mi R, Ye H, Zhang H, Chen B, Li Y, Huang G, Xia J (2019) Radiomics Nomogram Building From Multiparametric MRI to Predict Grade in Patients With Glioma: A Cohort Study. Journal of Magnetic Resonance Imaging: *JMRI,* ***49****(3): 825-833*.
18. Sun Z, Li Y, Wang Y, Fan X, Xu K, Wang K, Li S, Zhang Z, Jiang T, Liu X (2019) Radiogenomic analysis of vascular endothelial growth factor in patients with diffuse gliomas. *Cancer Imaging,* ***19****(1): 68*.
19. Jiang H, Chen X, Shi F, Ma Y, Xiang D, Ye L, Su J, Li Z, Chen Q, Hua Y, Xu X, Zhu W, Fan Y (2019) Improved cGAN based linear lesion segmentation in high myopia ICGA images. *Biomed Opt Express,* ***10*** *(5): 2355–2366*.
20. Konishi T (2015) Principal component analysis for designed experiments. *BMC Bioinformatics,* ***16****(18): S7*.
21. Hu W, Shen W, Zhou H, Kong D (2020) Matrix linear discriminant analysis. *Technometrics,* ***62(2):*** *196–205*.